Available online at http://ijim.srbiau.ac.ir/
Int. J. Industrial Mathematics (ISSN 2008-5621)
Vol. 10, No. 2, 2018 Article ID IJIM-00730, 14 pages
Research Article

Numerical Simulation of 1D Linear Telegraph Equation With Variable Coefficients Using Meshless Local Radial Point Interpolation (MLRPI)

E. Shivanian *†, S. Abbasbandy ‡, A. Khodayari §

Received Date: 2015-07-26 Revised Date: 2016-10-11 Accepted Date: 2017-10-16

Abstract

In the current work, we implement the meshless local radial point interpolation (MLRPI) method to find numerical solution of one-dimensional linear telegraph equations with variable coefficients. The MLRPI method, as a meshless technique, does not require any background integration cells and all integrations are carried out locally over small quadrature domains of regular shapes, such as lines in one dimensions, circles or squares in two dimensions and spheres or cubes in three dimensions. Weak form formulation of the discretized equations has been constructed on local subdomains, hence the domain and boundary integrals in the weak form methods can easily be evaluated over the regularly shaped sub-domains by some numerical quadratures. Radial basis functions augmented with monomials are used in to create shape functions. These shape functions have delta function property. Also the time derivatives is eliminated by using two-step finite differences approximation. Two illustrative numerical examples are given to show the stability and accuracy of the present method.

Keywords : Meshless local radial point interpolation (MLRPI); Radial basis function; Variable coefficient; Telegraph equation.

1 Introduction

This paper is dedicated to study the numerical solutions of the second order hyperbolic telegraph equation. The telegraph equation is important for modeling several relevant problems such as signal analysis [25], wave propagation [48], vibrational systems [10], random walk theory [6], mechanical systems [45] and etc. Recently, increasing attention has been paid to the development, analysis, and implementation of stable methods for the numerical solutions of second-order hyperbolic equations. There have been many numerical methods for hyperbolic equations, such as the finite difference, the finite element, and the collocation methods, etc. see [3, 4, 12, 11, 13, 14, 16, 17, 18, 24, 31, 32, 33, 34, 35, 46] and literatures are therein.

One of the most important advances in the field of numerical methods was the development

*Corresponding author. shivanian@sci.ikiu.ac.ir, Tel.:+98(912)6825371
†Department of Applied Mathematics, Imam Khomeini International University, Qazvin, Iran.
‡Department of Applied Mathematics, Imam Khomeini International University, Qazvin, Iran.
§Department of Applied Mathematics, Imam Khomeini International University, Qazvin, Iran.

of the finite element method (FEM) in the late 1950s. For a long time, FEM has been a standard tool for numerically solving different engineering problems. But The main shortcoming of FEM is that this numerical method rely on meshes or elements. Therefore, the meshless or meshfree method is proposed as one such numerical technique to overcome this shortcoming. Meshless methods have been developed in the past decade, and significant progress has been achieved recently for numerical computations of wide ranging engineering problems. These meshless methods do not require mesh for discretisation of problem domains, and they construct the approximate functions only via a set of nodes so-called field nodes where no element is required for approximation of functions [28]. In general, the meshless methods can be grouped into two categories based on using or not using integration or based on computational modelling [27]. The first category involves methods that do not require integration and are based on the strong forms of partial differential equations (PDEs) such as the meshless collocation method based on radial basis functions (RBFs) [26, 15, 29, 20] and the meshless collocation method based on boundary particle method (BPM) [21]. The second category includes meshless methods based on the weak forms of PDEs such as the element free Galerkin (EFG) method [8, 9]. In addition, a meshless method based on the combination of the strong form and weak form has also been developed and is known as the meshless weakstrong (MWS) form method. In the meshless strong form methods, usually the PDEs are discretized at nodes by the collocation technique and it is simple to implement. However, the meshless strong form methods have obvious shortcomings. For example, they are often numerically unstable and less accurate. The second category consists of meshless methods based on the weak forms of PDEs, including global weak form and local weak form. The meshless methods based on the weak form have very attractive merits. They exhibit very good stability and excellent accuracy. The reason is probably that the weak form can smear the computational error over the integral domain and control the error level [28]. The weak forms are used to derive a set of algebraic equations through a numerical integration process using a set of quadrature domain that may be constructed globally or locally in the domain of the problem. In the global weak form methods, global background cells are needed for numerical integration in computing the algebraic equations. To avoid the use of global background cells, a so-called local weak form is used to develop the meshless local Petrov-Galerkin (MLPG) and meshless local radial point interpolation (MLRPI) methods [44, 42, 43, 5, 41, 22, 1, 2, 38, 39, 40]. When a local weak form is used for a field node, the numerical integrations are carried out over a local quadrature domain defined for the node, which can also be the local domain where the test (weight) function is defined. The local domain usually has a regular and simple shape for an internal node (such as sphere, rectangular, etc.), and the integration is done numerically within the local domain. Hence the domain and boundary integrals in the weak form methods can easily be evaluated over the regularly shaped sub-domains(spheres in 3D or circles in 2D) and their boundaries.

According to the numerical results obtained by the MLRPI method, it seems this method can be employed as practical and effective numerical technique to solve telegraph equations with variable coefficients.

Let $\Omega = [0,1]$ and consider the 1D linear telegraph equation:

$$\frac{\partial^2 u(x,t)}{\partial t^2} + 2\alpha(x,t)\frac{\partial u(x,t)}{\partial t} + \beta^2(x,t)u(x,t) = A(x,t)\frac{\partial^2 u(x,t)}{\partial x^2} + g(x,t), \quad (x,t) \in \Omega \times [0,T], \tag{1.1}$$

with the initial and boundary conditions:

$$u(x,0) = g_1(x)\,, \ \frac{\partial u}{\partial t}(x,0) = g_2(x), \tag{1.2}$$

$$u(0,t) = \varphi_0(t)\,, \ u(1,t) = \varphi_1(t)\,, \ t \geq 0 \tag{1.3}$$

where $g, g_1, g_2, \varphi_0, \varphi_1$ are known functions, the function u is unknown and α, β, A are variable coefficients.

2 Numerical scheme

In this section, we concentrate on the numerical solution of the Eqs. (1.1)-(1.3) using the meshless local radial point interpolation (MLRPI) method.

2.1 Finite differences approximation

In the proposed method, we employ a time-stepping scheme to approximate the time derivative. For this purpose, the following finite difference approximations of order $O(\Delta t)^2$ are used:

$$\frac{\partial^2 u(\mathbf{x},t)}{\partial t^2} \cong \frac{1}{\Delta t^2}\Big(u^{(k+1)}(\mathbf{x}) - 2\,u^{(k)}(\mathbf{x}) + u^{(k-1)}(\mathbf{x})\Big), \tag{2.4}$$

$$\frac{\partial u(\mathbf{x},t)}{\partial t} \cong \frac{1}{2\,\Delta t}\Big(u^{(k+1)}(\mathbf{x}) - u^{(k-1)}(\mathbf{x})\Big). \tag{2.5}$$

By using Crank-Nicholson scheme, we have:

$$\begin{aligned} u(\mathbf{x},t) &\cong \frac{1}{3}\big(u^{(k+1)}(\mathbf{x}) + u^{(k)}(\mathbf{x}) \\ &+u^{(k-1)}(\mathbf{x})\big), \\ \frac{\partial^2 u(\mathbf{x},t)}{\partial \mathbf{x}^2} &\cong \frac{1}{3}\left(\frac{\partial^2 u^{(k+1)}(\mathbf{x},t)}{\partial \mathbf{x}^2}\right. \\ &\left.+\frac{\partial^2 u^{(k)}(\mathbf{x},t)}{\partial \mathbf{x}^2} + \frac{\partial^2 u^{(k-1)}(\mathbf{x},t)}{\partial \mathbf{x}^2}\right), \end{aligned} \tag{2.6}$$

where $u^k(\mathbf{x}) = u(\mathbf{x}, k\,\Delta t)$.
Using the above approximations, Eq. (1.1) becomes:

$$\begin{aligned} &\frac{1}{\Delta t^2}\big(u^{(k+1)}(\mathbf{x}) - 2\,u^{(k)}(\mathbf{x}) + u^{(k-1)}(\mathbf{x})\big) \\ &+\frac{\alpha}{\Delta t}\big(u^{(k+1)}(\mathbf{x}) - u^{(k-1)}(\mathbf{x})\big) \\ &+\frac{\beta^2}{3}\big(u^{(k+1)}(\mathbf{x}) + u^{(k)}(\mathbf{x}) + u^{(k-1)}(\mathbf{x})\big) \\ &-\frac{A}{3}\left(\frac{\partial^2 u^{(k+1)}(\mathbf{x})}{\partial \mathbf{x}^2} + \frac{\partial^2 u^{(k)}(\mathbf{x})}{\partial \mathbf{x}^2}\right. \\ &\left.+\frac{\partial^2 u^{(k-1)}(\mathbf{x})}{\partial \mathbf{x}^2}\right) \\ &= \frac{1}{3}\big(g^{(k+1)}(\mathbf{x}) + g^{(k)}(\mathbf{x}) + g^{(k-1)}(\mathbf{x})\big). \end{aligned} \tag{2.7}$$

In this paper for simplicity, telegraph equation is considered with variable coefficients $\alpha(x,t) = x^2, \beta(x,t) = x, A(x,t) = 1 + x$, therefore

$$\begin{aligned} &\frac{1}{\Delta t^2}\big(u^{(k+1)}(\mathbf{x}) - 2\,u^{(k)}(\mathbf{x}) + u^{(k-1)}(\mathbf{x})\big) \\ &+\frac{x^2}{\Delta t}\big(u^{(k+1)}(\mathbf{x}) - u^{(k-1)}(\mathbf{x})\big) \\ &+\frac{x^2}{3}\big(u^{(k+1)}(\mathbf{x}) + u^{(k)}(\mathbf{x}) + u^{(k-1)}(\mathbf{x})\big) \\ &-\frac{1+x}{3}\left(\frac{\partial^2 u^{(k+1)}(\mathbf{x})}{\partial \mathbf{x}^2} + \frac{\partial^2 u^{(k)}(\mathbf{x})}{\partial \mathbf{x}^2}\right. \\ &\left.+\frac{\partial^2 u^{(k-1)}(\mathbf{x})}{\partial \mathbf{x}^2}\right) \\ &= \frac{1}{3}\big(g^{(k+1)}(\mathbf{x}) + g^{(k)}(\mathbf{x}) + g^{(k-1)}(\mathbf{x})\big), \end{aligned} \tag{2.8}$$

thus

$$\begin{aligned} &\frac{1}{\Delta t^2}u^{(k+1)} + \left(\frac{1}{\Delta t} + \frac{1}{3}\right)x^2\,u^{(k+1)} \\ &-\frac{1}{3}\frac{\partial^2 u^{(k+1)}(\mathbf{x})}{\partial \mathbf{x}^2} - \frac{1}{3}\,x\,\frac{\partial^2 u^{(k+1)}(\mathbf{x})}{\partial \mathbf{x}^2} \\ &= \frac{2}{\Delta t^2}u^{(k)} - \frac{1}{3}x^2\,u^{(k)} \\ &+\frac{1}{3}\frac{\partial^2 u^{(k)}(\mathbf{x})}{\partial \mathbf{x}^2} + \frac{1}{3}\,x\,\frac{\partial^2 u^{(k)}(\mathbf{x})}{\partial \mathbf{x}^2} \\ &-\frac{1}{\Delta t^2}u^{(k-1)} + \left(\frac{1}{\Delta t} - \frac{1}{3}\right)x^2\,u^{(k-1)} \\ &+\frac{1}{3}\frac{\partial^2 u^{(k-1)}(\mathbf{x})}{\partial \mathbf{x}^2} + \frac{1}{3}\,x\,\frac{\partial^2 u^{(k-1)}(\mathbf{x})}{\partial \mathbf{x}^2} \\ &+\frac{1}{3}\big(g^{(k+1)}(\mathbf{x}) + g^{(k)}(\mathbf{x}) + g^{(k-1)}(\mathbf{x})\big). \end{aligned} \tag{2.9}$$

2.2 Approximation of field variables using radial point interpolation method

In the classical point interpolation method (PIM), we use monomial terms of a complete polynomail basis obtained from the triangle of pascal. It is possible that the polynomial moment matrix (it will be defined later) becomes singular or ill-conditioned, leading to the PIM failure. The most common reason for the inexistence of inverse of the polynomial moment matrix is the spatial collinearity of field nodes belonging to the same support-domain, which is recurrent in uniformly distributed nodal meshes or linear domain boundaries [7]. In order to avoid this drawback, the radial point interpolator (RPI) is employed. RPI is a numerical technique belonging to the point interpolation methods (PIM), which combines polynomial basis functions with radial basis

functions.
Consider a continuous function $u(x)$ defined in a domain Ω, which is represented by a set of field nodes. The $u(x)$ at a point of interest $\mathbf{x}$ is approximated in the form of

$$\begin{array}{c} u(\mathbf{x}) \;=\; \sum_{i=1}^{n} R_i(\mathbf{x})\, a_i \\ +\sum_{j=1}^{m} p_j(\mathbf{x})\, b_j \;=\; \mathbf{R}^T(\mathbf{x})\, \mathbf{a} \;+\; \mathbf{P}^T(\mathbf{x})\, \mathbf{b}, \end{array} \tag{2.10}$$

where $R_i(\mathbf{x})$ is a radial basis function (RBF), n is the number of RBFs, $p_j(\mathbf{x})$ is monomial in the space coordinate $\mathbf{x}$ and m is the number of polynomial basis functions. The $p_j(\mathbf{x})$ in Eq. (2.10) is, in general, chosen in a top-down approach from the Pascal triangle, so that the basis is complete to a desired order and a complete basis is usually preferred. For 1D problems, We use

$$\mathbf{P}^T(\mathbf{x}) \;=\; \{\, 1,\; x,\; x^2,\; x^3,\; ...,\; x^m \,\}, \tag{2.11}$$

for 2D problems, We shall have

$$\begin{array}{c} \mathbf{P}^T(\mathbf{x}) \;=\; \mathbf{P}^T(x,y) = \\ \{\, 1,\; x,\; y,\; xy,\; x^2,\; y^2,\; ...,\; x^m,\; y^m \,\}, \end{array} \tag{2.12}$$

and etc.
When $m = 0$, only RBFs are used. Otherwise, the RBF is augmented with m polynomial basis functions. Coefficients a_i and b_j are unknown which should be determined. There are a number of types of RBFs, and the characteristics of RBFs have been widely investigated [26, 19, 37]. In this paper we consider the thin plate spline (TPS) as radial basis functions in Eq. (2.10). This RBF is defined as follows:

$$R(\mathbf{x}) \;=\; r^{2s}\, \ln(r), \qquad s \;=\; 1,\; 2,\; 3,\; .... \tag{2.13}$$

Since $R(\mathbf{x})$ in Eq. (2.13) belongs to C^{2s-1} (all continuous function to the order $2s-1$), so higher-order thin plate splines must be used for higher-order partial differential operators. For the second-order partial differential equation (1.1), $s = 2$ is used for thin plate splines (i.e., second-order thin plate splines). In the radial basis function $R_i(\mathbf{x})$, the variable is only the distance between the point of interest $\mathbf{x}$ and a node at x_i, i.e., $r \;=\; |\; \mathbf{x} \;-\; x_i \;|$ for 1-D and $r \;=\; \sqrt{(\mathbf{x} \;-\; x_i)^2 \;+\; (\mathbf{y} \;-\; y_i)^2}$ for 2-D. In order to determine a_i and b_j in Eq. (2.10), a support domain is formed for the point of interest at $\mathbf{x}$, and n field nodes are included in the support domain. Coefficients a_i and b_j in Eq. (2.10) can be determined by enforcing Eq. (2.10) to be satisfied at these n nodes surrounding the point of interest $\mathbf{x}$. This leads to the system of n linear equations, one for each node. The matrix form of these equations can be expressed as

$$\mathbf{U}_s \;=\; \mathbf{R}_n\, \mathbf{a} \;+\; \mathbf{P}_m\, \mathbf{b}, \tag{2.14}$$

where the vector of function values U_s is

$$\mathbf{U}_s \;=\; \{\, u_1,\; u_2,\; u_3,\; ...,\; u_n \,\}^T, \tag{2.15}$$

the RBFs moment matrix is

$$\mathbf{R}_n \;=\; \left[\begin{array}{cccc} R_1(r_1) & R_2(r_1) & ... & R_n(r_1) \\ R_1(r_2) & R_2(r_2) & ... & R_n(r_2) \\ \vdots & \vdots & \ddots & \vdots \\ R_1(r_n) & R_2(r_n) & ... & R_n(r_n) \end{array}\right]_{n\times n}, \tag{2.16}$$

and the polynomial moment matrix is

$$\mathbf{P}_m \;=\; \left[\begin{array}{cccc} 1 & x_1 & ... & x_1^{m-1} \\ 1 & x_2 & ... & x_2^{m-1} \\ \vdots & \vdots & \ddots & \vdots \\ 1 & x_n & ... & x_n^{m-1} \end{array}\right]_{n\times m}. \tag{2.17}$$

Also, the vector of unknown coefficients for RBFs is

$$\mathbf{a}^T \;=\; \{\, a_1,\; a_2,\; a_3,\; ...,\; a_n \,\}, \tag{2.18}$$

and the vector of unknown coefficients for polynomial is

$$\mathbf{b}^T \;=\; \{\, b_1,\; b_2,\; b_3,\; ...,\; b_m \,\}. \tag{2.19}$$

We notify that, in Eq. (2.16), r_k in $R_i(r_k)$ is defined as

$$r_k \;=\; |\; \mathbf{x}_k \;-\; x_i \;|\,. \tag{2.20}$$

We mention that there are $m + n$ variables in Eq. (2.14). The additional m equations can be added using the following m constraint conditions:

$$\sum_{i=1}^{n} p_j(\mathbf{x}_i)\, a_i \;=\; \mathbf{P}_m^T\, \mathbf{a} \;=\; 0, \qquad j \;=\; 1,\; 2,\; ...,\; m. \tag{2.21}$$

Combining Eqs. (2.14) and (2.21) yields the following system of equations in the matrix form:

$$\tilde{\mathbf{U}}_s \;=\; \left[\begin{array}{c} \mathbf{U}_s \\ 0 \end{array}\right] \;=\; \left[\begin{array}{cc} \mathbf{R}_n & \mathbf{P}_m \\ \mathbf{P}_m^T & 0 \end{array}\right] \left[\begin{array}{c} \mathbf{a} \\ \mathbf{b} \end{array}\right] \;=\; \mathbf{G}\, \tilde{\mathbf{a}}, \tag{2.22}$$

where

$$\begin{aligned} \tilde{\mathbf{U}}_s^T &= \{\, u_1,\, u_2,\, ...,\, u_n,\, 0,\, 0,\, ...,\, 0 \,\}, \\ \tilde{\mathbf{a}}^T &= \{\, a_1,\, a_2,\, ...,\, a_n,\, b_1,\, ...,\, b_m \,\}. \end{aligned} \tag{2.23}$$

Because the matrix $\mathbf{R_n}$ is symmetric, the matrix $\mathbf{G}$ will also be symmetric. Solving Eq. (2.22), we obtain

$$\tilde{\mathbf{a}} = \begin{bmatrix} \mathbf{a} \\ \mathbf{b} \end{bmatrix} = \mathbf{G}^{-1}\, \tilde{\mathbf{U}}_s. \tag{2.24}$$

Eq. (2.10) can be rewritten as

$$u(\mathbf{x}) = \mathbf{R}^T(\mathbf{x})\, \mathbf{a} + \mathbf{P}^T(\mathbf{x})\, \mathbf{b} = \left\{\, \mathbf{R}^T(\mathbf{x}),\, \mathbf{P}^T(\mathbf{x}) \,\right\} \begin{bmatrix} \mathbf{a} \\ \mathbf{b} \end{bmatrix}. \tag{2.25}$$

Now using Eq. (2.24), we obtain

$$u(\mathbf{x}) = \left\{\mathbf{R}^T(\mathbf{x}), \mathbf{P}^T(\mathbf{x})\right\} \mathbf{G}^{-1} \tilde{\mathbf{U}}_s = \tilde{\Phi}^T(\mathbf{x}) \tilde{\mathbf{U}}_s, \tag{2.26}$$

where $\tilde{\Phi}^T(\mathbf{x})$ can be rewritten as

$$\tilde{\Phi}^T(\mathbf{x}) = \left\{\, \mathbf{R}^T(\mathbf{x}),\, \mathbf{P}^T(\mathbf{x}) \,\right\} \mathbf{G}^{-1} = \{\, \phi_1(\mathbf{x}),\, \phi_2(\mathbf{x}),\, ...,\, \phi_n(\mathbf{x}),\, \phi_{n+1}(\mathbf{x}),\, ...,\, \phi_{n+m}(\mathbf{x}) \,\}. \tag{2.27}$$

The first n functions of the above vector function are called the RPIM shape functions corresponding to the nodal displacements. We show by the vector $\tilde{\Phi}^T(\mathbf{x})$ so that it is

$$\tilde{\Phi}^T(\mathbf{x}) = \{\, \phi_1(\mathbf{x}),\, \phi_2(\mathbf{x}),\, ...,\, \phi_n(\mathbf{x}) \,\}. \tag{2.28}$$

Then Eq. (2.26) is converted to the following one:

$$u(\mathbf{x}) = \tilde{\Phi}^T(\mathbf{x})\, \tilde{\mathbf{U}}_s = \sum_{i=1}^{n} \phi_i(\mathbf{x})\, u_i. \tag{2.29}$$

The derivatives of $u(\mathbf{x})$ are easily obtained as

$$\begin{aligned} \frac{\partial u(\mathbf{x})}{\partial x} &= \sum_{i=1}^{n} \frac{\partial \phi_i(\mathbf{x})}{\partial x}\, u_i, \\ \frac{\partial^2 u(\mathbf{x})}{\partial x^2} &= \sum_{i=1}^{n} \frac{\partial^2 \phi_i(\mathbf{x})}{\partial x^2}\, u_i. \end{aligned} \tag{2.30}$$

Note that $\mathbf{R}_n^{-1}$ usually exists for arbitrary scattered nodes and therefore the augmented matrix $\mathbf{G}$ is theoretically non-singular [36, 47]. In addition, the order of polynomial used in Eq. (2.10) is relatively low. We add that the RPIM shape functions have the Kronecker delta function property, that is

$$\phi_i(\mathbf{x}_j) = \begin{cases} 1, & i = j, \quad j = 1, 2, ..., n, \\ 0, & i \neq j, \quad j = 1, 2, ..., n. \end{cases} \tag{2.31}$$

This is be cause the RPIM shape functions are created to pass through nodal values.

2.3 Local weak equations

To avoid the numerical integration on the whole domain, the MLRPI method constructs the weak form equations on local subdomains. The subdomains overlap with each other and cover the whole global domain. The subdomains could be of any geometric shape and size. In one dimensional problems, they are line (interval). For $\mathbf{x}_i$ in the interior of domain, we consider a subdomain Ω_q^i around $\mathbf{x}_i$, i.e, $\mathbf{x}_i \in \Omega_q^i = (x_i - r_q\, , x_i + r_q)$, and the local weak form of Eq. (2.9) for some test function ν on subdomain Ω_q^i will be written as follows:

$$\begin{aligned} &\frac{1}{\Delta t^2} \int_{\Omega_q^i} u^{(k+1)}\, \nu(\mathbf{x})\, dx + \left(\frac{1}{\Delta t} + \frac{1}{3}\right) \\ &\int_{\Omega_q^i} x^2 u^{(k+1)} \nu(\mathbf{x}) dx - \\ &\frac{1}{3} \int_{\Omega_q^i} \frac{\partial^2 u^{(k+1)}(\mathbf{x})}{\partial \mathbf{x}^2} \nu(\mathbf{x}) dx - \\ &\frac{1}{3} \int_{\Omega_q^i} x \frac{\partial^2 u^{(k+1)}(\mathbf{x})}{\partial \mathbf{x}^2} \nu(\mathbf{x}) dx = \\ &\frac{2}{\Delta t^2} \int_{\Omega_q^i} u^{(k)} \nu(\mathbf{x}) dx - \frac{1}{3} \int_{\Omega_q^i} x^2 u^{(k)} \nu(\mathbf{x}) dx \\ &+ \frac{1}{3} \int_{\Omega_q^i} \frac{\partial^2 u^{(k)}(\mathbf{x})}{\partial \mathbf{x}^2} \nu(\mathbf{x}) dx + \end{aligned} \tag{2.32}$$

$$\frac{1}{3}\int_{\Omega_q^i} x\frac{\partial^2 u^{(k)}(\mathbf{x})}{\partial \mathbf{x}^2}\nu(\mathbf{x})dx-$$

$$\frac{1}{\Delta t^2}\int_{\Omega_q^i} u^{(k-1)}\nu(\mathbf{x})dx$$

$$+\left(\frac{1}{\Delta t}-\frac{1}{3}\right)\int_{\Omega_q^i} x^2u^{(k-1)}\nu(\mathbf{x})dx+$$

$$\frac{1}{3}\int_{\Omega_q^i}\frac{\partial^2 u^{(k-1)}(\mathbf{x})}{\partial \mathbf{x}^2}\nu(\mathbf{x})dx$$

$$+\frac{1}{3}\int_{\Omega_q^i} x\frac{\partial^2 u^{(k-1)}(\mathbf{x})}{\partial \mathbf{x}^2}\nu(\mathbf{x})dx$$

$$+\frac{1}{3}\int_{\Omega_q^i}\left(g^{(k+1)}(\mathbf{x})+g^{(k)}(\mathbf{x})+g^{(k-1)}(\mathbf{x})\right)\times$$

$$\nu(\mathbf{x})dx,$$

using the Heaviside step function [23, 30]:

$$\nu(\mathbf{x})=\begin{cases}1, & x\in\Omega_q^i,\\ 0, & x\notin\Omega_q^i,\end{cases} \tag{2.33}$$

as the test function in each subdomain and using integration by parts:

$$\int_{\Omega_q^i}\frac{\partial^2 u^{(k)}(\mathbf{x})}{\partial \mathbf{x}^2}\nu(\mathbf{x})dx=$$

$$\nu(\mathbf{x})\frac{\partial u^{(k)}(\mathbf{x})}{\partial \mathbf{x}}\Big|_{\mathbf{x}=x_i-r_q}^{\mathbf{x}=x_i+r_q}- \tag{2.34}$$

$$\int_{\Omega_q^i}\frac{\partial u^{(k)}(\mathbf{x})}{\partial \mathbf{x}}\frac{\partial \nu(\mathbf{x})}{\partial x}dx,$$

$$\int_{\Omega_q^i} x\frac{\partial^2 u^{(k)}(\mathbf{x})}{\partial \mathbf{x}^2}\nu(\mathbf{x})dx=x\frac{\partial u^{(k)}(\mathbf{x})}{\partial \mathbf{x}}\Big|_{\mathbf{x}=x_i-r_q}^{\mathbf{x}=x_i+r_q}$$

$$-\int_{\Omega_q^i}\frac{\partial u^{(k)}(\mathbf{x})}{\partial \mathbf{x}}dx=x\frac{\partial u^{(k)}(\mathbf{x})}{\partial \mathbf{x}}\Big|_{\mathbf{x}=x_i-r_q}^{\mathbf{x}=x_i+r_q}$$

$$-u^{(k)}(\mathbf{x})\Big|_{\mathbf{x}=x_i-r_q}^{\mathbf{x}=x_i+r_q}, \tag{2.35}$$

the following local weak equation will be obtained:

$$\frac{1}{\Delta t^2}\int_{\Omega_q^i} u^{(k+1)}dx+\left(\frac{1}{\Delta t}+\frac{1}{3}\right)\int_{\Omega_q^i} x^2u^{(k+1)}dx$$

$$-\frac{1}{3}\left(\frac{\partial u^{(k+1)}(\mathbf{x})}{\partial \mathbf{x}}\Big|_{\mathbf{x}=x_i-r_q}^{\mathbf{x}=x_i+r_q}\right)$$

$$-\frac{1}{3}\left(x\frac{\partial u^{(k+1)}(\mathbf{x})}{\partial \mathbf{x}}\Big|_{\mathbf{x}=x_i-r_q}^{\mathbf{x}=x_i+r_q}\right)$$

$$+\frac{1}{3}\left(u^{(k+1)}\Big|_{\mathbf{x}=x_i-r_q}^{\mathbf{x}=x_i+r_q}\right)=$$

$$\frac{2}{\Delta t^2}\int_{\Omega_q^i} u^{(k)}dx-\frac{1}{3}\int_{\Omega_q^i} x^2u^{(k)}dx \tag{2.36}$$

$$+\frac{1}{3}\left(\frac{\partial u^{(k)}(\mathbf{x})}{\partial \mathbf{x}}\Big|_{\mathbf{x}=x_i-r_q}^{\mathbf{x}=x_i+r_q}\right)+$$

$$\frac{1}{3}\left(x\frac{\partial u^{(k)}(\mathbf{x})}{\partial \mathbf{x}}\Big|_{\mathbf{x}=x_i-r_q}^{\mathbf{x}=x_i+r_q}\right)-\frac{1}{3}\left(u^{(k)}\Big|_{\mathbf{x}=x_i-r_q}^{\mathbf{x}=x_i+r_q}\right)-$$

$$\frac{1}{\Delta t^2}\int_{\Omega_q^i} u^{(k-1)}dx+\left(\frac{1}{\Delta t}-\frac{1}{3}\right)\int_{\Omega_q^i} x^2u^{(k-1)}dx$$

$$+\frac{1}{3}\left(\frac{\partial u^{(k-1)}(\mathbf{x})}{\partial \mathbf{x}}\Big|_{\mathbf{x}=x_i-r_q}^{\mathbf{x}=x_i+r_q}\right)+$$

$$\frac{1}{3}\left(x\frac{\partial u^{(k-1)}(\mathbf{x})}{\partial \mathbf{x}}\Big|_{\mathbf{x}=x_i-r_q}^{\mathbf{x}=x_i+r_q}\right)$$

$$-\frac{1}{3}\left(u^{(k-1)}\Big|_{\mathbf{x}=x_i-r_q}^{\mathbf{x}=x_i+r_q}\right)+$$

$$\frac{1}{3}\int_{\Omega_q^i}\left(g^{(k+1)}(\mathbf{x})+g^{(k)}(\mathbf{x})+g^{(k-1)}(\mathbf{x})\right)dx.$$

Now, using the radial point interpolation (RPIM) shape functions the local integral equations (2.36) are transformed into a system of algebraic equations with respect to unknown quantities, as will be described in the next subsection.

2.4 Discretized equations

Now, we consider Eq. (2.36) to see how to obtain discrete equations. Consider N regularly

Table 1: The L^1, L^2 and L^∞ errors calculated by MLRPI for Example 3.1 with different Δx and Δt at time $t = 1.0$.

Δt	Δx	$\parallel E \parallel_1$	$\parallel E \parallel_2$	$\parallel E \parallel_\infty$
0.01	0.0125	$4.959087e-06$	$6.384063e-07$	$1.199214e-07$
0.0025	0.0125	$1.129247e-06$	$1.614878e-07$	$3.890040e-08$
0.00125	0.0125	$1.048819e-06$	$1.456785e-07$	$3.867238e-08$
0.001	0.0125	$1.039219e-06$	$1.439781e-07$	$3.864510e-08$

Table 2: The L^1, L^2 and L^∞ errors calculated by MLRPI for Example 3.1 with different Δx and Δt at time $t = 1.0$.

Δt	Δx	$\parallel E \parallel_1$	$\parallel E \parallel_2$	$\parallel E \parallel_\infty$
0.001	0.1	$6.589887e-04$	$2.605541e-04$	$1.755683e-04$
0.001	0.05	$7.800750e-05$	$2.191627e-05$	$1.136000e-05$
0.001	0.025	$8.830760e-06$	$1.738533e-06$	$6.605878e-07$
0.001	0.0125	$1.039219e-06$	$1.439781e-07$	$3.864510e-08$

Table 3: The L^1, L^2 and L^∞ errors calculated by MLRPI for Example 3.1 with different t at $\Delta x = 0.0125$ and $\Delta t = 0.001$

t	$\parallel E \parallel_1$	$\parallel E \parallel_2$	$\parallel E \parallel_\infty$
0.0	0	0	0
0.1	$1.358360e-07$	$1.778375e-08$	$3.079967e-09$
0.2	$2.645755e-07$	$3.365996e-08$	$5.625544e-09$
0.3	$3.623065e-07$	$4.541930e-08$	$7.216603e-09$
0.4	$4.089601e-07$	$5.129782e-08$	$7.964108e-09$
0.5	$3.984947e-07$	$5.046876e-08$	$8.134482e-09$
0.6	$3.485346e-07$	$4.463411e-08$	$7.832943e-09$
0.7	$3.031383e-07$	$4.146396e-08$	$1.283511e-08$
0.8	$3.239724e-07$	$5.573539e-08$	$1.947124e-08$
0.9	$5.787852e-07$	$9.146506e-08$	$2.795837e-08$
1.0	$1.039219e-06$	$1.439781e-07$	$3.864510e-08$

Table 4: The L^1, L^2 and L^∞ errors calculated by MLRPI for Example 3.2 with different Δx and Δt at time $t = 1.0$.

Δt	Δx	$\parallel E \parallel_1$	$\parallel E \parallel_2$	$\parallel E \parallel_\infty$
0.01	0.0125	$4.042456e-05$	$5.910543e-06$	$1.178377e-06$
0.0025	0.0125	$2.409794e-06$	$3.525553e-07$	$7.147390e-08$
0.00125	0.0125	$5.336124e-07$	$7.185181e-08$	$1.459832e-08$
0.001	0.0125	$3.400774e-07$	$4.333283e-08$	$7.754398e-09$

located points on the boundary and domain of the problem i.e. interval [0 1] so that the distance between two consecutive nodes in each direction is constant and equal to h. Assuming that $u(\mathbf{x}_i, k\Delta t), i = 1, 2, ..., N$ are known, our aim is to compute $u(\mathbf{x}_i, (k+1)\Delta t), i = 1, 2, ..., N$. So, we have N unknowns and to compute these unknowns, we need N equations. As it will be described, corresponding to each node we obtain one equation. To obtain the discrete equations from the locally weak forms (2.36), for nodes located in the interior of the domain, i.e., for $\mathbf{x}_i \in$ interior Ω, we substitute approximation formulas (2.29) and (2.30) into local integral equations

(2.36) to have

$$\frac{1}{\Delta t^2}\sum_{j=1}^{N}\left(\int_{\Omega_q^i}\phi_j(\mathbf{x})dx\right)u_j^{(k+1)}$$
$$+\left(\frac{1}{\Delta t}+\frac{1}{3}\right)\sum_{j=1}^{N}\left(\int_{\Omega_q^i}x^2\phi_j(\mathbf{x})dx\right)u_j^{(k+1)}$$
$$-\frac{1}{3}\sum_{j=1}^{N}\left(\frac{\partial\phi_j(\mathbf{x})}{\partial\mathbf{x}}\Big|_{\mathbf{x}=x_i+r_q}-\right.$$
$$\left.\frac{\partial\phi_j(\mathbf{x})}{\partial\mathbf{x}}\Big|_{\mathbf{x}=x_i-r_q}\right)u_j^{(k+1)}$$
$$-\frac{1}{3}\sum_{j=1}^{N}\left(x\frac{\partial\phi_j(\mathbf{x})}{\partial\mathbf{x}}\Big|_{\mathbf{x}=x_i+r_q}\right.$$
$$\left.-x\frac{\partial\phi_j(\mathbf{x})}{\partial\mathbf{x}}\Big|_{\mathbf{x}=x_i-r_q}\right)u_j^{(k+1)}$$
$$+\frac{1}{3}\sum_{j=1}^{N}\left(\phi_j(\mathbf{x})\Big|_{\mathbf{x}=x_i+r_q}\right.$$
$$\left.-\phi_j(\mathbf{x})\Big|_{\mathbf{x}=x_i-r_q}\right)u_j^{(k+1)}$$
$$=\frac{2}{\Delta t^2}\sum_{j=1}^{N}\left(\int_{\Omega_q^i}\phi_j(\mathbf{x})dx\right)u_j^{(k)}$$
$$-\frac{1}{3}\sum_{j=1}^{N}\left(\int_{\Omega_q^i}x^2\phi_j(\mathbf{x})dx\right)u_j^{(k)}$$
$$+\frac{1}{3}\sum_{j=1}^{N}\left(\frac{\partial\phi_j(\mathbf{x})}{\partial\mathbf{x}}\Big|_{\mathbf{x}=x_i+r_q}\right.$$
$$\left.-\frac{\partial\phi_j(\mathbf{x})}{\partial\mathbf{x}}\Big|_{\mathbf{x}=x_i-r_q}\right)u_j^{(k)}$$
$$+\frac{1}{3}\sum_{j=1}^{N}\left(x\frac{\partial\phi_j(\mathbf{x})}{\partial\mathbf{x}}\Big|_{\mathbf{x}=x_i+r_q}\right.$$
$$\left.-x\frac{\partial\phi_j(\mathbf{x})}{\partial\mathbf{x}}\Big|_{\mathbf{x}=x_i-r_q}\right)u_j^{(k)}$$
$$-\frac{1}{3}\sum_{j=1}^{N}\left(\phi_j(\mathbf{x})\Big|_{\mathbf{x}=x_i+r_q}\right.$$
$$\left.-\phi_j(\mathbf{x})\Big|_{\mathbf{x}=x_i-r_q}\right)u_j^{(k)}-$$
$$\frac{1}{\Delta t^2}\sum_{j=1}^{N}\left(\int_{\Omega_q^i}\phi_j(\mathbf{x})dx\right)u_j^{(k-1)}$$
$$+\left(\frac{1}{\Delta t}-\frac{1}{3}\right)\sum_{j=1}^{N}\left(\int_{\Omega_q^i}x^2\phi_j(\mathbf{x})dx\right)u_j^{(k-1)}$$
$$+\frac{1}{3}\sum_{j=1}^{N}\left(\frac{\partial\phi_j(\mathbf{x})}{\partial\mathbf{x}}\Big|_{\mathbf{x}=x_i+r_q}-\right.$$
$$\left.\frac{\partial\phi_j(\mathbf{x})}{\partial\mathbf{x}}\Big|_{\mathbf{x}=x_i-r_q}\right)u_j^{(k-1)}$$
$$+\frac{1}{3}\sum_{j=1}^{N}\left(x\frac{\partial\phi_j(\mathbf{x})}{\partial\mathbf{x}}\Big|_{\mathbf{x}=x_i+r_q}\right.$$
$$\left.-x\frac{\partial\phi_j(\mathbf{x})}{\partial\mathbf{x}}\Big|_{\mathbf{x}=x_i-r_q}\right)u_j^{(k-1)}$$
$$-\frac{1}{3}\sum_{j=1}^{N}\left(\phi_j(\mathbf{x})\Big|_{\mathbf{x}=x_i+r_q}-\right.$$
$$\left.\phi_j(\mathbf{x})\Big|_{\mathbf{x}=x_i-r_q}\right)u_j^{(k-1)}+$$
$$\frac{1}{3}\int_{\Omega_q^i}\left(g^{(k+1)}(\mathbf{x})+g^{(k)}(\mathbf{x})+g^{(k-1)}(\mathbf{x})\right)dx. \tag{2.37}$$

2.5 Implementation

For the boundary points, we have

$$\forall k: u^k(\mathbf{x}_1)=\varphi_0(k),\quad u^k(\mathbf{x}_N)=\varphi_1(k),$$
$$\mathbf{x}_i\in\partial\Omega=\{x_1=0,x_N=1\}. \tag{2.38}$$

The matrix forms of Eqs. (2.37) and (2.38) for all N nodal points in the domain and the boundary

of the problem are given below:

$$\begin{aligned}
&\Big[\tfrac{1}{\Delta t^2}\sum_{j=1}^{N}A_{i,j}+\left(\tfrac{1}{\Delta t}+\tfrac{1}{3}\right)\sum_{j=1}^{N}B_{i,j}\\
&-\tfrac{1}{3}\sum_{j=1}^{N}C_{i,j}-\tfrac{1}{3}\sum_{j=1}^{N}D_{i,j}+\tfrac{1}{3}\sum_{j=1}^{N}E_{i,j}\Big]\\
u_j^{(k+1)}=&\Big[\tfrac{2}{\Delta t^2}\sum_{j=1}^{N}A_{i,j}-\tfrac{1}{3}\sum_{j=1}^{N}B_{i,j}+\\
&\tfrac{1}{3}\sum_{j=1}^{N}C_{i,j}+\tfrac{1}{3}\sum_{j=1}^{N}D_{i,j}-\tfrac{1}{3}\sum_{j=1}^{N}E_{i,j}\Big]\\
&u_j^{(k)}+\Big[-\tfrac{1}{\Delta t^2}\sum_{j=1}^{N}A_{i,j}+\left(\tfrac{1}{\Delta t}-\tfrac{1}{3}\right)\sum_{j=1}^{N}B_{i,j}\\
&+\tfrac{1}{3}\sum_{j=1}^{N}C_{i,j}+\tfrac{1}{3}\sum_{j=1}^{N}D_{i,j}-\tfrac{1}{3}\sum_{j=1}^{N}E_{i,j}\Big]\\
&u_j^{(k-1)}+F_i(k-1,k,k+1),
\end{aligned}\tag{2.39}$$

where

$$\begin{aligned}
&A_{i,j}=\textstyle\int_{\Omega_q^i}\phi_j(\mathbf{x})dx,\\
&B_{i,j}=\textstyle\int_{\Omega_q^i}x^2\phi_j(\mathbf{x})dx,\\
&C_{i,j}=\left(\frac{\partial\phi_j(\mathbf{x})}{\partial\mathbf{x}}\Big|_{\mathbf{x}=x_i+r_q}-\frac{\partial\phi_j(\mathbf{x})}{\partial\mathbf{x}}\Big|_{\mathbf{x}=x_i-r_q}\right),\\
&D_{i,j}=\left(x\frac{\partial\phi_j(\mathbf{x})}{\partial\mathbf{x}}\Big|_{\mathbf{x}=x_i+r_q}-x\frac{\partial\phi_j(\mathbf{x})}{\partial\mathbf{x}}\Big|_{\mathbf{x}=x_i-r_q}\right),\\
&E_{i,j}=\left(\phi_j(\mathbf{x})\Big|_{\mathbf{x}=x_i+r_q}-\phi_j(\mathbf{x})\Big|_{\mathbf{x}=x_i-r_q}\right),\\
&F_i(k-1,k,k+1)=\frac{1}{3}\textstyle\int_{\Omega_q^i}\\
&\left(g^{(k+1)}(\mathbf{x})+g^{(k)}(\mathbf{x})+g^{(k-1)}(\mathbf{x})\right)dx.
\end{aligned}\tag{2.40}$$

Assuming

$$\begin{aligned}
\mathbf{A}_{i,j}=&\tfrac{1}{\Delta t^2}A_{i,j}+\left(\tfrac{1}{\Delta t}+\tfrac{1}{3}\right)B_{i,j}\\
&-\tfrac{1}{3}C_{i,j}-\tfrac{1}{3}D_{i,j}+\tfrac{1}{3}E_{i,j},\\
\mathbf{B}_{i,j}=&\tfrac{2}{\Delta t^2}A_{i,j}-\tfrac{1}{3}B_{i,j}+\tfrac{1}{3}C_{i,j}+\\
&\tfrac{1}{3}D_{i,j}-\tfrac{1}{3}E_{i,j},
\end{aligned}\tag{2.41}$$

$$\begin{aligned}
\mathbf{C}_{i,j}=&-\tfrac{1}{\Delta t^2}A_{i,j}+\left(\tfrac{1}{\Delta t}-\tfrac{1}{3}\right)B_{i,j}+\\
&\tfrac{1}{3}C_{i,j}+\tfrac{1}{3}D_{i,j}-\tfrac{1}{3}E_{i,j},\\
\mathbf{F}^k=&[F_1(k-1,k,k+1),\\
&F_2(k-1,k,k+1),...,F_N(k-1,k,k+1)]^T,\\
U=&[u_1,u_2,...,u_N]^T,
\end{aligned}$$

yeilds

$$\mathbf{A}U^{(k+1)}=\mathbf{B}U^{(k)}+\mathbf{C}U^{(k-1)}+\mathbf{F}^k.\tag{2.42}$$

Furthermore, to satisfy Eqs. (2.38), for both nodes belong to the boundary, i.e., $\{x_1,x_N\}$, we set

$$\forall k:\mathbf{F}_i^k=\varphi_i(k),\forall j:\mathbf{B}_{i,j}=\mathbf{C}_{i,j}=0,$$

$$\mathbf{A}_{i,j}=\begin{cases}1,i=j,\\0,i\neq j.\end{cases}\tag{2.43}$$

At the first time level, when $k=0$, according to the initial conditions that were introduced in Eq. (1.2), we apply the following assumptions:

$$u^{(0)}=g_1(x),$$

and

$$u^{(-1)}\cong u^{(1)}-2\Delta t g_2(x),$$

where $g_1(x)=[g_1(x_1),g_1(x_2),...,g_1(x_N)]^T$ and $g_2(x)=[g_2(x_1),g_2(x_2),...,g_2(x_N)]^T$.

3 Numerical demonstrations

The proposed MLRPI scheme is applied to two numerical examples of 1D linear telegraph equation with variable coefficients. In the current work a uniform node arrangement, with step size $h=\Delta x$ is used. To numerical investigation of the local technique it is important to generate the local sub-domain for each computational node, in our process we construct the local quadrature domain by choosing $r_q=0.8h$, where r_q is the radius of local subdomain. The size of r_q is such that the union of these sub-domains must cover the whole global domain. In the process, the 7 point Gauss quadrature rule is used to evaluate the domain integrals. The radius of support domain to local radial point interpolation method is $r_s=4r_q$.

This size is significant enough to have sufficient number of nodes (n) to give appropriate shape functions. Also, in Eq. (2.10), we set $m = 5$.

Example 3.1 *Consider the telegraph equation (1) with variable coefficients $\alpha = x^2$, $\beta = x$ and $A = 1 + x$ over the domain [0 , 1] with the following initial and boundary conditions:*

$$u(x,0) = 0, \qquad \frac{\partial u}{\partial t}(x,0) = 0,$$

$$u(0,t) = 0, \qquad u(1,t) = 0, \qquad t \geq 0.$$

The exact solution is given by

$$u(x,t) = t^3x^2(1-x)^2, \qquad (x,t) \in [0,1] \times [0,1]$$

and

$$g(x,t) = (6t + 6x^2t^2 + x^2t^3)x^2(1-x)^2$$

$$-t^3(1+x)(2 - 12x + 12x^2).$$

The results of the example are reported in Tables 1, 2 and 3 and Fig f1. As it is seen, MLRPI method is of high accuracy. Also Tables 1 and 2 show the order of convergence of the scheme. It can be seen that the errors are decreasing as we decrease Δt or Δx.]

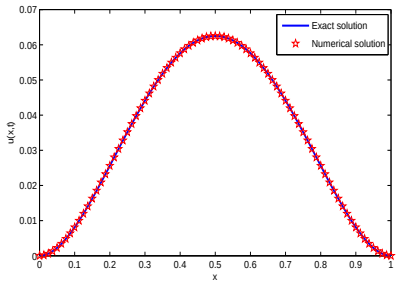

Figure 1: Numerical solutions and exact solution at time $t = 1.0$ for Example 3.1. The solid line corresponds to the exact solution, the stared line corresponds to numerical solution of the MLRPI with $\Delta t = 0.001$ and $\Delta x = 0.0125$.

Example 3.2 *In this example, telegraph equation (1) is considered with variable coefficients $\alpha = x^2$, $\beta = x$ and $A = 1+x$ over the domain [0 , 1] and following initial and boundary conditions:*

$$u(x,0) = 0, \qquad \frac{\partial u}{\partial t}(x,0) = 0,$$

$$u(0,t) = 0, \qquad u(1,t) = 0, \qquad t \geq 0.$$

The exact solution is given by

$$u(x,t) = t^2(1-x)sinh(x), \quad (x,t) \in [0,1] \times [0,1]$$

and

$$g(x,t) = (2 + 4x^2t + x^2t^2 - t^2 - xt^2)\times$$

$$(1-x)sinh(x) + (2t^2 + 2xt^2)cosh(x).$$

The results of the example are reported in Tables 4, 5 and 6 and Fig 2. As it is seen, MLRPI method is of high accuracy. Also Tables 4 and 5 show the order of convergence of the scheme. It can be seen again the errors are decreasing as we decrease Δt or Δx.

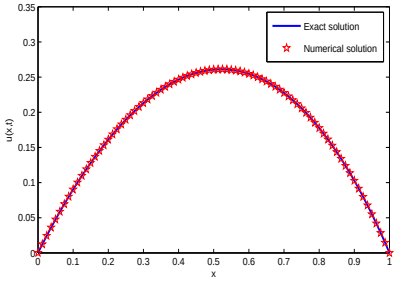

Figure 2: Numerical solutions and exact solution at time $t = 1.0$ for Example 3.2. The solid line corresponds to the exact solution, the stared line corresponds to numerical solution of the MLRPI with $\Delta t = 0.001$ and $\Delta x = 0.0125$.

4 Conclusions

In this article, The meshless local radial point interpolation (MLRPI) method has been formulated and successfully implemented for solving the linear telegraph equation with variable coefficients. The time variable has been discretized by using finite differences approximation. Also, weak form of the discretized equations has been constructed on local subdomains. Furthermore, The radial point interpolation method is adopted for approximating the field variables. All integrations are regular, therefore the Gaussian quadrature rule used to calculate the numerical integration for local weak form.
The proposed method is a truly meshless method,

Table 5: The L^1, L^2 and L^∞ errors calculated by MLRPI for Example 3.2 with different Δx and Δt at time $t = 1.0$.

Δt	Δx	$\| E \|_1$	$\| E \|_2$	$\| E \|_\infty$
0.001	0.1	$2.284578e-04$	$7.702824e-05$	$3.246693e-05$
0.001	0.05	$2.576054e-05$	$6.007151e-06$	$1.877456e-06$
0.001	0.025	$2.893497e-06$	$4.757451e-07$	$1.179273e-07$
0.001	0.0125	$3.400774e-07$	$4.333283e-08$	$7.754398e-09$

Table 6: The L^1, L^2 and L^∞ errors calculated by MLRPI for Example 2 with different t at $\Delta x = 0.0125$ and $\Delta t = 0.001$.

t	$\| E \|_1$	$\| E \|_2$	$\| E \|_\infty$
0.0	0	0	0
0.1	$3.880335e-07$	$5.440162e-08$	$1.023566e-08$
0.2	$6.507940e-07$	$8.805265e-08$	$1.624005e-08$
0.3	$7.864868e-07$	$1.015752e-07$	$1.793090e-08$
0.4	$8.207701e-07$	$1.028369e-07$	$1.752439e-08$
0.5	$7.763044e-07$	$9.760137e-08$	$1.707048e-08$
0.6	$6.652667e-07$	$8.486414e-08$	$1.555002e-08$
0.7	$4.956624e-07$	$6.144735e-08$	$1.096194e-08$
0.8	$2.870293e-07$	$3.243863e-08$	$4.663845e-09$
0.9	$2.130055e-07$	$2.736595e-08$	$5.918456e-09$
1.0	$3.400774e-07$	$4.333283e-08$	$7.754398e-09$

which requires neither domain elements nor background cells in either the interpolation or the integration. The main advantage of the scheme is to capture the behaviour of solution for similar problems with variable coefficients where most of the schemes fail. Test problems verified the accuracy and convergency of the proposed approach.

References

[1] S. Abbasbandy, HR. Ghehsareh, I Hashim, Ameshfree method for the solution of two-dimensional cubic nonlinear Schrödinger equation, *Engineering Analysis with Boundary Elements* 37 (2013) 885-898.

[2] S. Abbasbandy, HR. Ghehsareh, I Hashim, Numerical analysis of a mathematical model for capillary formation in tumor angiogenesis using ameshfree method based on the radial basis function, *Engineering Analysis with Boundary Elements* 36 (2012) 1811-1818.

[3] P. Almenar, L. Jodar, J.A. Martin, Mixed problems for the time-dependent telegraph equation: Continuous numerical solutions with a priori error bounds, *Math. Comput. Modelling* 25 (1997) 31-44.

[4] R. Aloy, M. C. Casabn, L.A. Caudillo-Mata, L. Jdar, Computing the variable coefficient telegraph equation using a discrete eigenfunction method, *Comput. Math. Appl.* 54 (2007) 448-458.

[5] M. Aslefallah, E. Shivanian, E. Nonlinear fractional integro-differential reaction-diffusion equation via radial basis functions, *The European Physical Journal Plus* 130 (2015) 1-9.

[6] J. Banasiak, J. R. Mika, Singularly perturbed telegraph equations with applications in the random walk theory, *J. Appl. Math. Stoch. Anal.* 11 (1998) 9-28.

[7] J. Belinha, Meshless methods in biomechanics, Springer International Publishing Switzerland, 2014.

[8] T. Belytschko, Y. Y. Lu, L. Gu, Element-free Galerkin methods. *International Journal for Numerical Methods in Engineering* 37 (1994) 229-256.

[9] T. Belytschko, Y. Y. Lu, L. Gu, Element free Galerkin methods for static and dynamic fracture, *International Journal of Solids and Structures* 32 (1995) 2547-2570.

[10] W. E. Boyce, R. C. DiPrima, Differential Equations Elementary and Boundary Value Problems, Wiley, New York, 1977.

[11] M. Ciment, S.H. Leventhal, A note on the operator compact implicit method for the wave equation, *Math. Comp.* 32 (1978) 143-147.

[12] M. Ciment, S. H. Leventhal, Higher order compact implicit schemes for the wave equation, *Math. Comp.* 29 (1975) 985-994.

[13] G. Dahlquist, On accuracy and unconditional stability of linear multi-step methods for second order differential equations, *BIT* 18 (1978) 133-136.

[14] M. Dehghan, A. Mohebbi, High order implicit collocation method for the solution of two-dimensional linear hyperbolic equation, *Numer. Methods PDEs* 25 (2009) 232-243.

[15] M. Dehghan, A. Shokri, A numerical method for solution of the two dimensional sine-Gordon equation using the radial basis functions, *Mathematics and Computers inSimulation* 79 (2008) 700-715.

[16] M. Dehghan, A. Shokri, A numerical method for solving the hyperbolic telegraph equation, *Numer. Methods PDEs* 24 (2008) 1080-1093.

[17] H. Ding, Y. Zhang, A new fourth-order compact finite difference scheme for the two-dimensional second-order hyperbolic equation, *J. Comp. Appl. Math.* 230 (2009) 626-632.

[18] M. S. El-Azab, M. El-Gamel, A numerical algorithm for the solution of telegraph equations, *Appl. Math. Comput.* 190 (2007) 757-764.

[19] C. Franke, R. Schaback, Solving partial differential equations by collocation using radial basis functions, *Applied Mathematics and Computation* 93 (1997) 73-82.

[20] Z. J. Fu, W. Chen, L. Ling. Method of approximate particular solutions for constant- and variable-order fractional diffusion models, *Eng. Anal. Boundary Elem.* 57 (2015) 37-46.

[21] Z. J. Fu, W. Chen, H.T. Yang. Boundary particle method for Laplace transformed time fractional diffusion equations, *Journal of Computational Physics* 235 (2013) 52-66.

[22] VR. Hosseini, E. Shivanian, W. Chen, Local integration of 2-D fractional telegraph equation via local radial point interpolant approximation, *The European Physical Journal Plus* 130 (2015) 1-21.

[23] D. Hu, S. Long, K. Liu, G. Li, A modified meshless local Petrov-Galerkin method to elasticity problems in computer modeling and simulation, *Engineering Analysis with Boundary Elements* 30 (2006) 399-404.

[24] L. Jdar, D. Goberna, Analytic-numerical solution with a priori error bounds for coupled time-dependent telegraph equations: Mixed problems, *Math Comput. Modelling* 30 (1999) 39-53.

[25] P. M. Jordan, A. Puri, Digital signal propagation in dispersive media, *J. Appl. Phys.* 85 (1999) 1273-1282.

[26] E. Kansa, Multiquadrics-a scattered data approximation scheme with applications to computational fluid-dynamics. I. Surface approximations and partial derivative estimates *Computers & Mathematics with Applications* 19 (1990) 127-145.

[27] S. F. Li, W. K. Liu, Meshfree and particle methods and their application, *Applied Mechanics Reviews* 55 (2002) 1-34.

[28] H. Li, S. S. Mulay, Meshless methods and their numerical properties, CRC Press, Taylor and Francies Group, 2013

[29] J. Lin, W. Chen, K. Y. Sze, A new radial basis function for Helmholtz problems, *Engineering Analysis with Boundary Elements* 36 (2012) 1923-1930.

[30] K. Liu, S. Long, G. Li, A simple and less-costly meshless local Petrov-Galerkin (MLPG) method for the dynamic fracture problem, *Engineering Analysis with Boundary Elements* 30 (2006) 72-76.

[31] R. K. Mohanty, An unconditionally stable difference scheme for the one-space dimensional linear hyperbolic equation, *Appl. Math. Lett.* 17 (2004) 101-105.

[32] R. K. Mohanty, M. K. Jain, An unconditionally stable alternating direction implicit scheme for the two space dimensional linear hyperbolic equation, *Numer. Methods PDEs* 17 (2001) 684-688.

[33] R. K. Mohanty, M. K. Jain, U. Arora, An unconditionally stable ADI method for the linear hyperbolic equation in three space dimensions, *Int. J. Comput. Math.* 79 (2002) 133-142.

[34] R. K. Mohanty, M. K. Jain, K. George, High order difference schemes for the system of two space second order nonlinear hyperbolic equations with variable coefficients, *J. Comp. Appl. Math.* 70 (1996) 231-243.

[35] R. K. Mohanty, M. K. Jain, K. George, On the use of high order difference methods for the system of one space second order nonlinear hyperbolic equations with variable coefficients, *J. Comp. Appl. Math.* 72 (1996) 421-431.

[36] M. J. D. Powell, Theory of radial basis function approximation in 1990, in: F.W. Light (Ed.), *Adv. Numer. Anal.* (1992) 303-322.

[37] M. Sharan, E. J. Kansa, S. Gupta, Application of the multiquadric method for numerical solution of elliptic partial differential equations, *Appl. Math. Comput.* 84 (1997) 275-302.

[38] A. Shirzadi, L. Ling, S. Abbasbandy, Meshlesss imulations of the two-dimensional fractional-time convection-diffusion-reaction equations, *Engineering Analysis with Boundary Elements* 36 (2012) 1522-1527.

[39] A. Shirzadi, V. Sladek, J. Sladek, A local integral equation formulation to solve coupled nonlinear reaction-diffusion equations by using moving least square approximation, *Engineering Analysis with Boundary Elements* 37 (2013) 8-14.

[40] E. Shivanian, A new spectral meshless radial point interpolation (SMRPI)method: a well-behaved alternative to themeshlessweak forms, Engineering Analysis with Boundary Elements 54 (2015) 1-12.

[41] E. Shivanian, S. Abbasbandy, MS. Alhuthali, HH. Alsulami, Local integration of 2-D fractional telegraph equation via moving least squares approximation, *Engineering Analysis with Boundary Elements* 56 (2015) 98-105.

[42] E. Shivanian, Analysis of meshless local radial point interpolation (MLRPI) on a nonlinear partial integro-differential equation arising in population dynamics, *Engineering Analysis with Boundary Elements* 37 (2013) 1693-1702.

[43] E. Shivanian, On the convergence analysis, stability, and implementation of meshless local radial point interpolation on a class of three-dimensional wave equations, *International Journal for NumericalMethods in Engineering* (in press) 2015. http://dx.doi.org/10.1002/nme.4960./

[44] E. Shivanian, HR. Khodabandehlo, Meshless local radial point interpolation (MLRPI) on the telegraph equation with purely integral conditions, *European Physical Journal* 129 (2014) 241-251.

[45] A. N. Tikhonov, A. A. Samarskii, Equations of Mathematical Physics, Dover, New York, 1990.

[46] E. H. Twizell, An explicit difference method for the wave equation with extended stability range, *BIT* 19 (1979) 378-383.

[47] H. Wendland, Error estimates for interpolation by compactly supported radial basis functions of minimal degree, *Journal of Approximation Theory* 93 (1998) 258-396.

[48] V. H. Weston, S. He, Wave splitting of the telegraph equation in R^3 and its application to inverse scattering, *Inverse Problems*, 9 (1993) 789-812.

Dr. Elyas Shivanian was born in Zanjan province, Iran in August 26, 1982. He started his master course in applied mathematics in 2005 at Amirkabir University of Technology and has finished MSc. thesis in the field of fuzzy linear programming in 2007. His research interests are analytical and numerical solutions of ODEs, PDEs and IEs. He has published several papers on these subjects. He also has published some papers in other fields, for more information see please http://scholar.google.com/citations?user=MFncks8AAAAJ&hl=en

Saeid Abbasbandy has got PhD degree from Kharazmi University in 1996 and now he is the full professor in Imam Khomeini International University, Ghazvin, Iran. He has published more than 300 papers in international journals and conferences. Now, he is working on numerical analysis and fuzzy numerical analysis.

Arman Khodayari was born in Kermanshah province, Iran on September 21, 1988. I started my master course in applied mathematics in 2013 at Alborz University and have finished MSc. Thesis in the field of numerical solution of partial differential equations. I became member of Irans National Elites Foundation in 2017. My interest is meshless methods.